



Research article

Advantages of fluid and white matter suppression (FLAWS) with MP2RAGE compared with double inversion recovery turbo spin echo (DIR-TSE) at 7T



Yuta Urushibata^{a,1}, Hideto Kuribayashi^{a,1,*}, Koji Fujimoto^b, Tobias Kober^{c,d,e}, John W Grinstead^f, Tadashi Isa^{b,g}, Tomohisa Okada^b

^a Siemens Healthcare K.K., Tokyo, Japan

^b Human Brain Research Center, Graduate School of Medicine, Kyoto University, Kyoto, Japan

^c Advanced Clinical Imaging Technology, Siemens Healthcare AG, Lausanne, Switzerland

^d Department of Radiology, University Hospital (CHUV), Lausanne, Switzerland

^e LTS5, École Polytechnique Fédérale de Lausanne (EPFL), Lausanne, Switzerland

^f Siemens Healthcare USA, Portland, USA

^g Department of Neuroscience, Graduate School of Medicine, Kyoto University, Kyoto, Japan

ARTICLE INFO

Keywords:

Double inversion recovery
FLAWS
MP2RAGE
MRI
7T

ABSTRACT

Cerebrospinal fluid (CSF) and white matter (WM) signal suppression techniques allow better visualization of both WM and gray matter (GM) lesions in such disorders as multiple sclerosis and epilepsy. Recently, a technique, FLuid And White matter Suppression “FLAWS”, has been proposed at 3T based on the magnetization-prepared with two rapid gradient echoes (MP2RAGE) sequence. In this study, the FLAWS-MP2RAGE pulse sequence was compared with a double inversion recovery turbo spin echo (DIR-TSE) sequence at 7T. Twenty-two healthy volunteers were examined. Isotropic spatial resolution of 1 mm and a scan time of approximately 6 min were chosen due to a restricted clinical schedule. Homogeneity of CSF and WM signal suppression was compared with GM signal as an intensity reference. Volumes of GM visualization and specific absorption rates (SARs) were compared using Wilcoxon-rank sum tests with Bonferroni-Holm correction for multiple comparisons. WM-to-GM signal ratios in FLAWS-MP2RAGE images were significantly lower than DIR-TSE (median: 24.5% vs 59.0%, $P < 0.0001$), whereas CSF-to-GM signal ratios in FLAWS-MP2RAGE were significantly higher than DIR-TSE (57.1% vs 38.3%, $P = 0.0001$). Ranges of the signal ratios between 20 and 80 percentiles were lower in FLAWS-MP2RAGE than DIR-TSE for WM (24.1% vs 37.2%, $P < 0.0001$) but were higher in FLAWS-MP2RAGE compared with DIR-TSE for CSF (80.8% vs 63.0%, $P = 0.0001$). Pixels of low GM signal ($< 20\%$ of the median) were mainly distributed at the skull base, and these low signal GM volume ratios were lower in FLAWS-MP2RAGE than DIR-TSE (2.27% vs 6.18%, $P < 0.0001$). Median SAR in sixteen subjects was 2.5 times higher in DIR-TSE than in FLAWS-MP2RAGE. FLAWS-MP2RAGE showed superior and more homogenous WM signal suppression, better GM visualization at the skull base and lower SAR compared with DIR-TSE, suggesting superiority of FLAWS-MP2RAGE at 7T.

1. Introduction

Cerebrospinal fluid (CSF) and white matter (WM) signal suppression techniques are known to increase gray matter (GM) and WM lesion conspicuity for detecting multiple sclerosis [1–3] and epilepsy [4–6]. Double inversion recovery (DIR) is a well-known technique to suppress both of those signals simultaneously [1,5,6]. The application at ultra-high field (UHF) MRI is attractive because of increased signal-to-noise ratio and typically higher spatial resolution, which are crucial for

imaging small and/or ambiguous lesions. Three dimensional (3D) T₂-weighted DIR pulse sequences have previously been applied to multiple sclerosis at 7 Tesla (7T) [7,8]. Unexpectedly, the 3D DIR sequence showed worse [7] to only comparable [8] lesion conspicuity compared to a 3D fluid attenuated inversion recovery sequence. Moreover, its introduction into clinical 7T MRI protocols may be difficult because its scan time is longer than 10 min when high spatial resolution is prioritized.

A new technique, FLuid And White matter Suppression “FLAWS”,

* Corresponding author at: Siemens Healthcare K.K., 1-11-1 Osaki, Shinagawa-ku, Tokyo, 141-8644, Japan.

E-mail address: hideto.kuribayashi@siemens-healthineers.com (H. Kuribayashi).

¹ These authors contributed equally to this work.

has recently been proposed at 3 Tesla (3 T) based on the magnetization-prepared with two rapid gradient echoes (MP2RAGE) sequence [9]. The MP2RAGE pulse sequence acquires two 3D gradient-recalled echo (GRE) images with different inversion times (TIs) to compute a B_1 field insensitive T_1 -weighted image [10] and a quantitative T_1 map [11] useful for tissue segmentation [12,13] and investigation of physiological [14] or pathological changes [15]. In the FLAWS-MP2RAGE [9], two TIs are set to null WM and CSF signals in the first and second GRE images, respectively. The FLAWS contrast is computed by combining minimum values of the two. To suppress both CSF and WM at UHF MRI, an MP2RAGE sequence may be advantageous over a TSE-based DIR sequence for which two inversion pulses and a train of refocusing pulses are required which imposes a higher specific absorption rate (SAR).

In this study, we investigated both DIR-TSE and FLAWS-MP2RAGE 3D sequences at 7 T, and compared suppression of CSF and WM, GM delineation, and SAR in healthy volunteers using statistical analysis. Signal intensities of DIR-TSE and FLAWS-MP2RAGE as a function of T_1 were simulated to validate optimized scan parameters.

2. Material and methods

2.1. Image acquisition

Twenty-two healthy volunteers (15 males and 7 females, mean age 29.5 years, aged 20–51 years) were examined using a 7 T scanner (MAGNETOM 7T, Siemens Healthcare, Erlangen, Germany) equipped with a whole-body gradient system (70 m T/m maximum amplitude, 200 m T/m/ms maximum slew rate). A single-channel volume transmit coil with a 32-channel phased array receiver head coil was used (Nova Medical, MA, USA). The study was approved by institutional review board, and written informed consent was obtained by all subjects. Both DIR-TSE and FLAWS-MP2RAGE were prototype sequences provided by the MRI vendor. Inversion times (TI1 and TI2) of DIR-TSE sequence were defined as delays from the start of the first and the second non-selective adiabatic inversion pulses of 10.24-ms pulse width to the start of the excitation pulse for 3D TSE readout, respectively. The corresponding TIs of FLAWS-MP2RAGE sequence were defined as delays from the start of the adiabatic inversion pulse [16] to the acquisition of the center of k-space by each of the two 3D GRE readouts.

To facilitate clinical applications, both DIR-TSE and FLAWS-MP2RAGE scans were conducted with isotropic spatial resolution of 1 mm and a scan time of approximately 6 min. Identical imaging parameters for those sequences were: field-of-view = 192×192 (mm)², matrix size = 192×192 , number of slices = 192, slice thickness = 1 mm, orientation = sagittal, generalized auto-calibrating partially parallel acquisition (GRAPPA) acceleration factor = 3. The TSE sequence was based on SPACE (sampling perfection with application optimized contrasts by using different flip angle evolutions) [17] with elliptical 3D k-space sampling. Flip angle evolution of the refocusing pulse train was generated for T_2 -weighted contrast of target tissues having $T_1/T_2 = 1450/75$ ms and an apparent echo time (TE) = 93 ms. DIR-TSE parameters were: repetition time (TR) = 6 s, TE = 299 ms, bandwidth = 579 Hz/pixel, echo train length = 222, echo-spacing = 3.36 ms. FLAWS-MP2RAGE parameters were: TR = 5 s, TE = 2.05 ms, flip angles for the two GRE readouts = 4° and 5°, bandwidth = 410 Hz/pixel, and fat signal suppressed. FLAWS-MP2RAGE contrast images were reconstructed online. The TIs were empirically optimized so that signal from both CSF and WM was minimized with volunteer scans prior to this comparative study. The optimal TI1/TI2 were 2670/450 ms at TR = 6 s for DIR-TSE, and those were 700/1700 ms at TR = 5 s for FLAWS-MP2RAGE sequence. Local SAR in the head was recorded at the end of the scans.

For brain segmentation to GM, WM and CSF, classical T_1 -weighted images were obtained using a prototype MPRAGE pulse sequence with an adiabatic inversion pulse optimized for 7 T [16] and double-echo of TEs = 2.08 and 5.77 ms for signal averaging. Other MPRAGE

parameters were: TR = 2.3 s, TI = 1050 ms, flip angle = 6°, FOV = 206×206 (mm)², matrix size = 256×256 , slice thickness = 0.8 mm (i.e., 0.8-mm isotropic resolution), number of slices = 224, orientation = sagittal, bandwidth = 420 Hz/pixel, and GRAPPA acceleration factor = 3. In all volunteer scans, ears and the back of the head were covered with dielectric pads of CaTiO₃ suspension in D₂O (40% v/v) [18] to mitigate B_1 inhomogeneity.

2.2. Image analysis

Image post-processing was carried out using SPM12 (<http://www.fil.ion.ucl.ac.uk/spm/>) implemented in MATLAB (MathWorks, MA, USA). Images of DIR-TSE and FLAWS-MP2RAGE were registered to the corresponding T_1 -weighted MPRAGE images in each subject. The T_1 -weighted images were normalized to MNI standard brain space [19], and the derived parameters of the normalization were applied to the images of the DIR-TSE and the FLAWS-MP2RAGE. The normalized T_1 -weighted images were segmented to GM, WM and CSF. The normalized DIR-TSE and FLAWS-MP2RAGE images were segmented to GM, WM and CSF with the regions segmented on the normalized T_1 -weighted images. GM, WM and CSF signals on the segmented DIR-TSE and FLAWS-MP2RAGE images in each subject were measured. To evaluate signal suppression, WM and CSF signal compared with GM signal as an intensity reference (i.e., WM-to-GM, CSF-to-GM) were calculated for each subject. At 7 T, transmit RF field inhomogeneity is larger than at 3 T, which causes signal inhomogeneity. To evaluate signal suppression homogeneity, the difference between the 20th and 80th percentile values of the signal ratios WM-to-GM and CSF-to-GM, were calculated for each subject. Low signal intensity regions in GM caused by signal inhomogeneity were considered inappropriate for evaluation and treated as signal defects, which were defined as voxels where the signal intensity was lower than 20 percent of the median of segmented GM values. GM signal defect ratio was calculated as the volume of GM signal defect divided by the total GM volume in each subject.

The measured values were checked for the distributional assumption of normality using Shapiro-Wilk test. The difference in mean or median measured value was compared between those sequences. Analyses were conducted using either paired *t*-test or Wilcoxon-rank sum test for normally or non-normally distributed values, respectively. A *P* value less than 0.05 was considered significant after Bonferroni-Holm correction for multiple comparisons. MedCalc (MedCalc version 18, Ostend, Belgium) was used for the analysis.

2.3. Simulation

In order to validate optimized scan parameters at 7 T, signal intensity for FLAWS-MP2RAGE as a function of T_1 was simulated based on the formula in [11], and signal intensity for DIR-TSE with T_2 -weighting effect from the apparent TE [20]. T_2 was assumed to be 20 times shorter than T_1 in this simulation for the DIR-TSE sequence. T_2 and T_2^* values were not taken into account in this simulation for the FLAWS-MP2RAGE sequence.

3. Results

Kolmogorov-Smirnov tests rejected normal distribution of all of the measured values in statistical analysis, thus median and non-parametric test were used for evaluation. Fig. 1 shows DIR-TSE (left) and FLAWS-MP2RAGE (right) images of an exemplary subject. WM was better suppressed in FLAWS-MP2RAGE than DIR-TSE. For quantitative evaluation of tissue signal intensity, images were segmented to GM, WM and CSF. Fig. 2 shows maps of segmented tissues of GM (dark gray), WM (light gray) and CSF (black) on DIR-TSE (top) and FLAWS-MP2RAGE (bottom) images calculated from the corresponding normalized and segmented T_1 -weighted images of the subject for Fig. 1. WM-to-GM signal ratios in FLAWS-MP2RAGE images were significantly

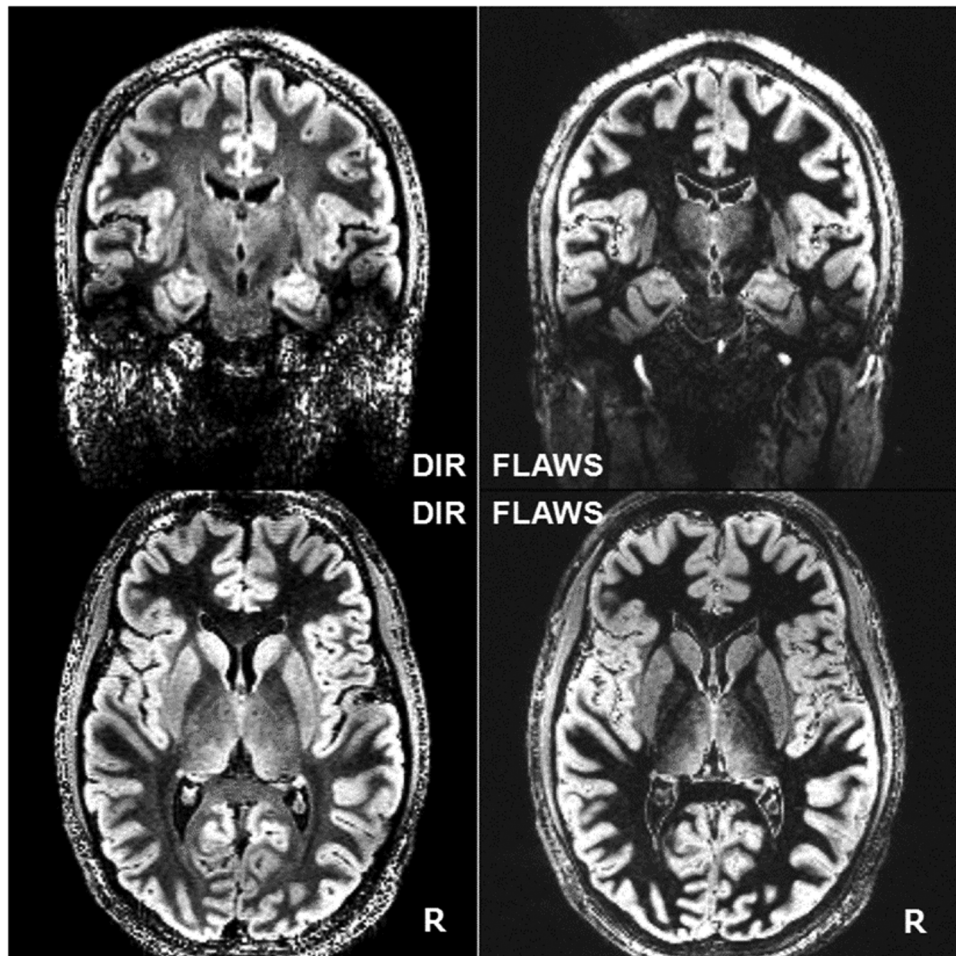


Fig. 1. Representative fluid and white matter suppressed MR images at 7T. Double inversion recovery turbo spin echo (DIR-TSE, left), fluid and white matter suppression magnetization-prepared with two rapid gradient echoes (FLAWS-MP2RAGE, right).

lower (median: 24.5% [95% confidence intervals: 23.6–26.5%]) than those in DIR-TSE images (59.0% [56.3–62.5%], $P < 0.0001$). On the other hand, CSF-to-GM signal ratios in FLAWS-MP2RAGE images were significantly higher (57.1% [52.6–60.0%]) than those in DIR-TSE images (38.3% [37.3–41.4%], $P = 0.0001$).

To evaluate signal suppression homogeneity, the difference between the 20th and 80th percentile values of the WM-to-GM and CSF-to-GM values for each subject was measured. The difference values in FLAWS-MP2RAGE were significantly lower (24.1% [22.5–25.6%]) than those in DIR-TSE (37.2% [32.7–39.7%], $P < 0.0001$) for WM, but they were significantly higher in FLAWS-MP2RAGE (80.8% [77.8–84.1%]) than those in DIR-TSE (63.0% [61.0–70.7%], $P = 0.0001$) for CSF.

In the analysis of signal defect that was defined as lower values than 20% of median values, signal defect GM pixels were mainly distributed at the skull base, represented as white pixels in Fig. 2. Signal defect GM volumes compared with total GM volumes (%) in FLAWS-MP2RAGE images were significantly lower than those in DIR-TSE images (2.27% [2.01–2.55%] vs 6.18% [5.81–6.81%], $P < 0.0001$).

The SAR values are subject dependent and are presented on the scan software as a percentage of the maximum SAR allowed for the head. The values were manually recorded in 16 cases. Median local SAR values (%) were 62.5% (52.2–71.2%) and 25.5% (22.0–29.4%) in DIR-TSE and FLAWS-MP2RAGE scans respectively, and the former was 2.5 times higher.

Simulated DIR-TSE and FLAWS-MP2RAGE image intensities as a function of T_1 using the optimized scan parameters mentioned above are presented in Fig. 3a and b, respectively. The DIR-TSE signal intensity was zero at $T_1 = 670$ ms. Beyond that point, the signal intensity

dramatically increases to a peak at $T_1 = 1.9$ s and then goes to zero at $T_1 = 5$ s. The FLAWS-MP2RAGE signal intensity goes to zero at $T_1 = 1150$ ms. Beyond that point, the signal intensity increases to a peak at $T_1 = 3.2$ s and then decreases. The nulled T_1 value in the FLAWS-MP2RAGE is in close agreement with published T_1 for WM at 7 T (ca. 1150 ms in [11], 1200 ms in [15], 1220 ms in [21]).

4. Discussion

This technical evaluation study clarified that FLAWS-MP2RAGE was superior to DIR-TSE in terms of better and more homogenous WM suppression, i.e., higher GM-to-WM contrast, more homogenous GM delineation, less signal defect volumes in GM, and lower SAR. On the other hand, DIR-TSE was superior to FLAWS-MP2RAGE in terms of better and more homogenous CSF suppression.

It is challenging to obtain high quality images using pulse sequences requiring large flip angle RF pulses on UHF MR systems, especially for an inversion pulse that requires a large bandwidth to compensate more severe B_0 inhomogeneity effects at UHF. It is also difficult to attain high inversion efficiency across the whole brain within allowed SAR levels. In this respect, the FLAWS-MP2RAGE sequence having a single inversion pulse preparation and small flip angle GRE readout is advantageous compared to the DIR-TSE sequence having two inversion pulses preparation and large flip angle TSE readout. As a result, the DIR-TSE images exhibited non-uniformity of both WM suppression and GM delineation in whole brain. The inferior part of the head in the DIR-TSE images was affected, which is visible in the coronal view of Fig. 1. This was aggravated by the use of a local single-channel volume RF transmit

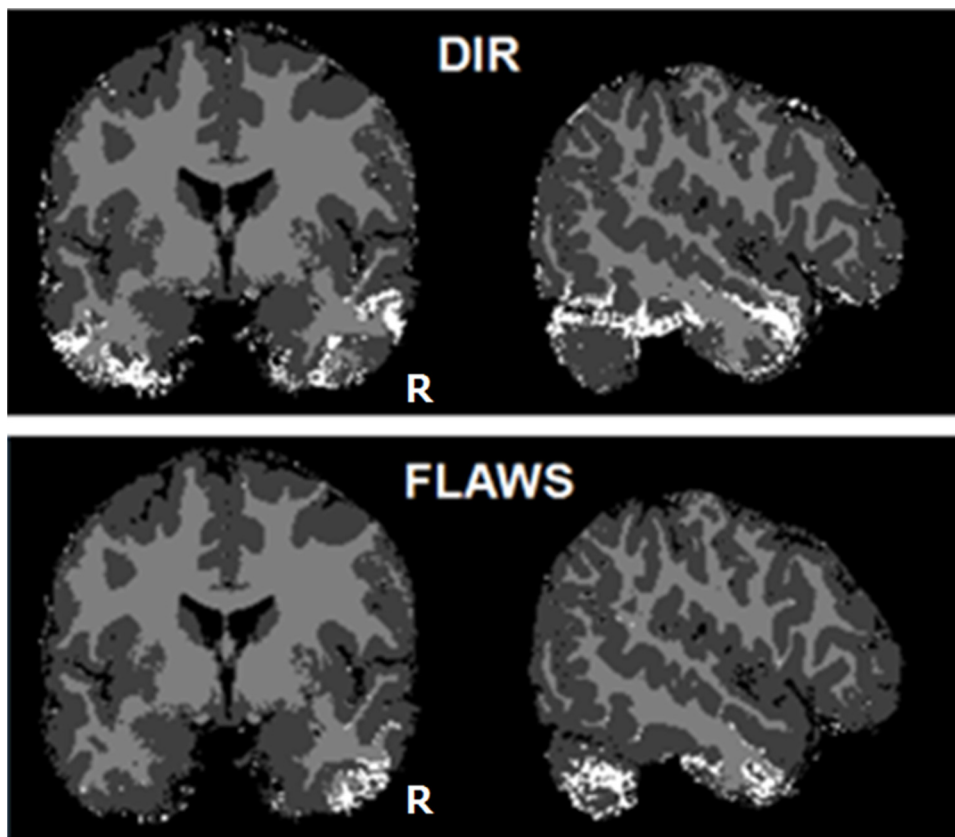


Fig. 2. Segmented maps of the subject for Fig. 1. Gray matter (dark gray), white matter (light gray) and cerebrospinal fluid (black) calculated from the normalized images of double inversion recovery turbo spin echo (DIR-TSE, top) and of fluid and white matter suppression magnetization-prepared with two rapid gradient echoes (FLAWS-MP2RAGE, bottom). Signal defect gray matter pixels (white) were mainly distributed at the skull base.

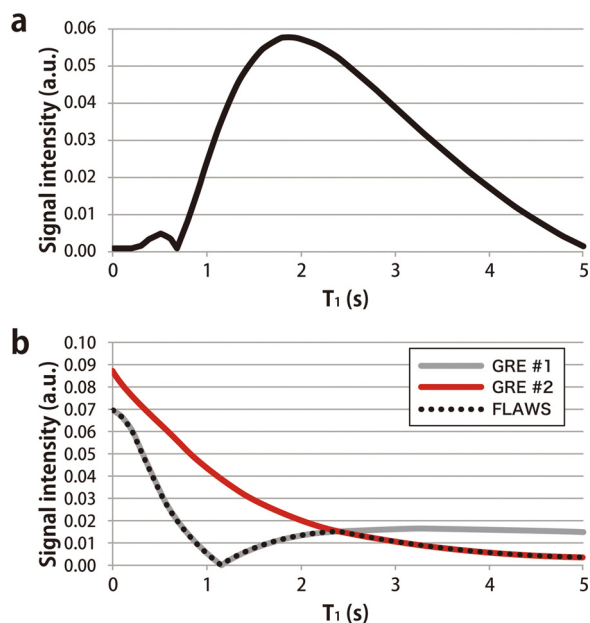


Fig. 3. Simulated image intensity of the fluid and white matter suppression pulse sequences as a function of T_1 . (a) Double inversion recovery turbo spin echo (DIR-TSE). (b) Fluid and white matter suppression magnetization-prepared with two rapid gradient echoes (FLAWS-MP2RAGE). The vertical scales are not consistent in arbitrary unit. Gradient-recalled echo (GRE) #1 and #2 are the first and the second GRE in MP2RAGE sequence. Optimized scan parameters were used. T_2 was assumed to be 20 times shorter than T_1 in this simulation for the DIR-TSE sequence. T_2 and T_2^* values were not taken into account in this simulation for the FLAWS-MP2RAGE sequence. Published T_1 values for white matter, gray matter, and cerebrospinal fluid at 7 T were ca. 1.2 s, 1.7–2.1 s, and 4.4 s, respectively [11,15,21].

coil that has a relatively short homogenous region of B_1 field along the Z-direction as well as its perpendicular directions due to shortening of its wavelength at 7 T.

High spatial resolution is one of the appeals of UHF MR imaging, but long scan time can limit the practical gains. The longer T_1 of tissues at 7 T compared to lower magnetic fields can lead to longer optimal TR and TI which can increase scan time. It took longer than 10 min per 3D DIR pulse sequence protocol with TR = 8 s reported in [7,8]. We could optimize the 1-mm isotropic 3D pulse sequences as 6-minute scans with the shorter TR (6 s) and GRAPPA acceleration (factor = 3). The scan time reduction in the FLAWS-MP2RAGE pulse sequence was accomplished with shortening TR (5 s) because of its low RF power requirement. Advanced fast imaging techniques other than GRAPPA for 3D acquisition, such as compressed sensing, could further reduce scan time for both DIR-TSE and FLAWS-MP2RAGE.

Superior signal suppression for both WM and CSF were not accomplished with empirical optimization. Although both of the two TIs affect the signal null points, it was straightforward to inspect WM suppression in FLAWS-MP2RAGE using the first TI GRE images. In DIR-TSE sequence, it was more difficult to find a signal null point for WM T_1 while maintaining CSF signal suppression whose signal tended to be high in the T_2 -weighted contrast.

The original study of FLAWS-MP2RAGE at 3 T [9] was conducted with volunteers as in this study, and detected WM lesions were reported as an incidental finding. The WM lesions were seen as hyper-intensity in the first TI GRE and reconstructed FLAWS images, and as hypo-intensity in the second TI GRE images, i.e. conventional T_1 -weighted MPRAGE. Their simulation study suggested that the WM lesion was depicted as a result of increased T_1 . Cortical lesion detection is another purpose to use CSF- and WM-suppressed imaging sequences. In the study of cortical lesion detection using MP2RAGE at 7 T [15], mean T_1 values were much higher in juxtacortical (2062 ± 230 ms) and slightly higher in intracortical (1871 ± 96 ms) lesions than in normal-appearing GM (1703 ± 90 ms). The DIR-TSE sequence is expected to generate slightly

higher signal intensity for such lesions compared with normal-appearing GM as simulated in Fig. 3, although further studies should evaluate this in patients. However, the image contrast especially in small objects may be degraded by partial volume effects in TSE [17]. Thus, FLAWS-MP2RAGE may be advantageous in depicting small lesions and lesion borders.

5. Conclusions

The FLAWS-MP2RAGE sequence showed better and more uniform WM suppression, more homogeneous GM delineation, and lower SAR compared with the DIR-TSE sequence which had better and more uniform CSF suppression at 7 T. This study suggests the FLAWS-MP2RAGE sequence may prove to be a better candidate for WM and cortical lesion detection with highly resolved observation at UHF MR.

Funding

This work was supported by a governmental grant from METI/JETRO Subsidy Program for Global Innovation Centers.

Declaration of interest statement

The following authors, Yuta Urushibata, Hideto Kuribayashi, Tobias Kober and John W. Grinstead are employees of Siemens Healthcare in their local countries and in charge of designing this study. Data acquisition, data analysis and simulation were conducted by the rest of the authors.

Acknowledgements

The authors thank Drs. Bénédicte Maréchal and Paul Dominik (Siemens Healthineers) to develop the pulse sequences, Junko Inoue MBA (Siemens Healthcare K.K., Japan) to manage the program, and Mr. Satoru Shimosako (Siemens Healthcare K.K., Japan) to help graph drawing.

References

- [1] B. Simon, S. Schmidt, C. Lukas, J. Gieseke, F. Träber, D.L. Knol, et al., Improved in vivo detection of cortical lesions in multiple sclerosis using double inversion recovery MR imaging at 3 tesla, *Eur. Radiol.* 20 (2010) 1675–1683, <https://doi.org/10.1007/s00330-009-1705-y>.
- [2] E.C. Tallantyre, P.S. Morgan, J.E. Dixon, A. Al-Radaideh, M.J. Brookes, P.G. Morris, et al., 3 tesla and 7 tesla MRI of multiple sclerosis cortical lesions, *J. Magn. Reson. Imaging* 32 (2010) 971–977, <https://doi.org/10.1002/jmri.22115>.
- [3] F. Nelson, A. Poonawalla, S. Datta, J. Wolinski, P. Narayana, Is 3D MPRAGE better than the combination DIR/PSIR for cortical lesion detection at 3 T MRI? *Mult. Scler. Relat. Disord.* 3 (2014) 253–257, <https://doi.org/10.1016/j.msard.2013.10.002>.
- [4] E. Morimoto, M. Kanagaki, T. Okada, A. Yamamoto, N. Mori, R. Matsumoto, et al., Anterior temporal lobe white matter abnormal signal (ATLAS) as an indicator of seizure focus laterality in temporal lobe epilepsy: comparison of double inversion recovery, FLAIR and T2W MR imaging, *Eur. Radiol.* 23 (2013) 3–11, <https://doi.org/10.1007/s00330-012-2565-4>.
- [5] E. Morimoto, T. Okada, M. Kanagaki, A. Yamamoto, Y. Fushimi, R. Matsumoto, et al., Evaluation of focus laterality in temporal lobe epilepsy: a quantitative study comparing double inversion-recovery MR imaging at 3T with FDG-PET, *Epilepsia* 54 (2013) 2174–2183, <https://doi.org/10.1111/epi.12396>.
- [6] L.C. Wong-Kisiel, J.W. Britton, R.J. Witte, K.M. Kelly-Williams, A.L. Kotsenas, K.N. Krecke, et al., Double inversion recovery magnetic resonance imaging in identifying focal cortical dysplasia, *Pediatr. Neurol.* 61 (2016) 87–93, <https://doi.org/10.1016/j.pediatrneurol.2016.04.013>.
- [7] I.D. Kilsdonk, W.L. de Graaf, A.L. Soriano, J.J. Zwanenburg, F. Visser, J.P. Kuijter, et al., Multicontrast MR imaging at 7T in multiple sclerosis: highest lesion detection in cortical gray matter with 3D-FLAIR, *AJNR* 34 (2013) 791–796, <https://doi.org/10.3174/ajnr.A3289>.
- [8] W.L. de Graaf, J.J. Zwanenburg, F. Visser, M.P. Wattjes, P.J. Pouwels, J.J. Geurts, et al., Lesion detection at seven tesla in multiple sclerosis using magnetisation prepared 3D-FLAIR and 3D-DIR, *Eur. Radiol.* 22 (2012) 221–231, <https://doi.org/10.1007/s00330-011-2242-z>.
- [9] M. Tanner, G. Gambarota, T. Kober, G. Krueger, D. Erritzoe, J.P. Marques, et al., Fluid and white matter suppression with the MP2RAGE sequence, *J. Magn. Reson. Imaging* 35 (2012) 1063–1070, <https://doi.org/10.1002/jmri.23532>.
- [10] P.-F. Van de Moortele, E.J. Auerbach, C. Olman, E. Yacoub, K. Ugurbil, S. Moeller, T₁ weighted brain images at 7 tesla unbiased for proton density, T₂* contrast and RF coil receive B₁ sensitivity with simultaneous vessel visualization, *Neuroimage* 46 (2009) 432–446, <https://doi.org/10.1016/j.neuroimage.2009.02.009>.
- [11] J.P. Marques, T. Kober, G. Krueger, W. van der Zwaag, P.F. Van de Moortele, R. Gruetter, MP2RAGE, a self bias-field corrected sequence for improved segmentation and T₁-mapping at high field, *Neuroimage* 49 (2010) 1271–1281, <https://doi.org/10.1016/j.neuroimage.2009.10.002>.
- [12] P.-L. Bazin, M. Weiss, J. Dinse, A. Schäfer, R. Trampel, R. Turner, A computational framework for ultra-high resolution cortical segmentation at 7 tesla, *Neuroimage* 93 (2014) 201–209, <https://doi.org/10.1016/j.neuroimage.2013.03.077>.
- [13] G. Okubo, T. Okada, A. Yamamoto, M. Kanagaki, Y. Fushimi, T. Okada, et al., MP2RAGE for deep gray matter measurement of the brain: a comparative study with MPRAGE, *J. Magn. Reson. Imaging* 43 (2016) 55–62, <https://doi.org/10.1002/jmri.24960>.
- [14] G. Okubo, T. Okada, A. Yamamoto, Y. Fushimi, T. Okada, K. Murata, et al., Relationship between aging and T₁ relaxation time in deep gray matter: a voxel-based analysis, *J. Magn. Reson. Imaging* 46 (2017) 724–731, <https://doi.org/10.1002/jmri.25590>.
- [15] E.S. Beck, P. Sati, V. Sethi, T. Kober, B. Dewey, P. Bhargava, et al., Improved visualization of cortical lesions in multiple sclerosis using 7T MP2RAGE, *Am. J. Neuroradiol.* 39 (2018) 459–466, <https://doi.org/10.3174/ajnr.A5534>.
- [16] K.R. O'Brien, A.W. Magill, J. Delacoste, J.P. Marques, T. Kober, H.-P. Fautz, et al., Dielectric pads and low-B₁⁺ adiabatic pulses: complementary techniques to optimize structural T₁w whole-brain MP2RAGE scans at 7 tesla, *J. Magn. Reson. Imaging* 40 (2014) 804–812, <https://doi.org/10.1002/jmri.24435>.
- [17] J.P. Mugler 3rd, Optimized three-dimensional fast-spin-echo MRI, *J. Magn. Reson. Imaging* 39 (2014) 745–767, <https://doi.org/10.1002/jmri.24542>.
- [18] W. Luo, M.T. Lanagan, C.T. Sica, Y. Ryu, S. Oh, M. Ketterman, et al., Permittivity and performance of dielectric pads with sintered ceramic beads in MRI: early experiments and simulations at 3T, *Magn. Reson. Med.* 270 (2013) 269–275, <https://doi.org/10.1002/mrm.24433>.
- [19] A.C. Evans, A.L. Janke, D.L. Collins, S. Baillet, Brain templates and atlases, *Neuroimage* 62 (2012) 911–922, <https://doi.org/10.1016/j.neuroimage.2012.01.024>.
- [20] S.J.P. Meara, G.J. Barker, Evolution of the longitudinal magnetization for pulse sequences using a fast spin-echo readout: application to fluid-attenuated inversion-recovery and double inversion-recovery sequences, *Magn. Reson. Med.* 54 (2005) 241–245, <https://doi.org/10.1002/mrm.20541>.
- [21] W.D. Rooney, G. Johnson, X. Li, E.R. Cohen, S.G. Kim, K. Ugurbil, et al., Magnetic field and tissue dependencies of human brain longitudinal ¹H₂O relaxation in vivo, *Magn. Reson. Med.* 57 (2007) 308–318, <https://doi.org/10.1002/mrm.21122>.